Mannose-Binding Lectin Drives Platelet Inflammatory Phenotype and Vascular Damage After Cerebral Ischemia in Mice via IL (Interleukin)-1α

Franca Orsini,* Stefano Fumagalli,* Eszter Császár, Krisztina Tóth, Daiana De Blasio, Rosalia Zangari, Nikolett Lénárt, Ádám Dénes, Maria-Grazia De Simoni

Objective—Circulating complement factors are activated by tissue damage and contribute to acute brain injury. The deposition of MBL (mannose-binding lectin), one of the initiators of the lectin complement pathway, on the cerebral endothelium activated by ischemia is a major pathogenic event leading to brain injury. The molecular mechanisms through which MBL influences outcome after ischemia are not understood yet.

Approach and Results—Here we show that MBL-deficient (MBL$^{-/-}$) mice subjected to cerebral ischemia display better flow recovery and less plasma extravasation in the brain than wild-type mice, as assessed by in vivo 2-photon microscopy. This results in reduced vascular dysfunction as shown by the shift from a pro- to an anti-inflammatory vascular phenotype associated with MBL deficiency. We also show that platelets directly bind MBL and that platelets from MBL$^{-/-}$ mice have reduced inflammatory phenotype as indicated by reduced IL-1α (interleukin-1α) content, as early as 6 hours after ischemia. Cultured human brain endothelial cells subjected to oxygen-glucose deprivation and exposed to platelets from MBL$^{-/-}$ mice present less cell death and lower CXCL1 (chemokine [C-X-C motif] ligand 1) release (downstream to IL-1α) than those exposed to wild-type platelets. In turn, MBL deposition on ischemic vessels significantly decreases after ischemia in mice treated with IL-1 receptor antagonist compared with controls, indicating a reciprocal interplay between MBL and IL-1α facilitating endothelial damage.

Conclusions—We propose MBL as a hub of pathogenic vascular events. It acts as an early trigger of platelet IL-1α release, which in turn favors MBL deposition on ischemic vessels promoting an endothelial pro-inflammatory phenotype.

Visual Overview—An online visual overview is available for this article. (*Arterioscler Thromb Vasc Biol*. 2018;38:2678-2690. DOI: 10.1161/ATVBAHA.118.311058.)

Key Words: endothelium ■ interleukin-1 ■ mannose-binding lectin ■ platelets ■ stroke

Clinical and experimental evidence indicates that the complement system, a powerful arm of the inflammatory response, is involved in stroke pathophysiology.[1–3] Available evidence points to the lectin pathway (LP), one of the activation pathways of the complement system, as a major contributor to the progression of brain damage.[4–6] In mice, targeting one of the LP initiator molecules, MBL (mannose-binding lectin), by pharmacological inhibition or genetic deletion reduces injury.[5,6] Notably in ischemic stroke patients, MBL deficiency is associated with smaller lesion and better outcome,[5,7] highlighting the relevance of MBL role in human brain ischemia.

Immunofluorescence studies in ischemic mice reveal that MBL is selectively deposited on the ischemic endothelium for several hours after injury and at least up to 48 hours and this deposition is reduced in mice treated with the MBL inhibitor Polyman 2.[6] MBL deposition on the activated endothelium is consistent with its ability to recognize and bind epitopes exposed on the surface of damaged cells.[8,9] The target molecules recognized by MBL on the activated endothelium and the mechanisms by which MBL deposited on the activated endothelium contribute to brain injury are unknown. MBL and the LP not only drive the activation of the complement cascade leading to inflammation, phagocytosis, and possibly lysis of target cells but also display a high degree of interaction with coagulation and kinin systems.[10–14] Activation of these cascades results in increased inflammation, blood clotting, and vascular permeability, further contributing to brain damage.[12] Thus, MBL deposition on the ischemic endothelium seems to act as a hub of several crucial events contributing to ischemic injury.

Nonstandard Abbreviations and Acronyms	
hBMEC	human brain microvascular endothelial cells
ICAM-1	intracellular adhesion molecule-1
IL-1R1	interleukin-1 receptor
IL-1Ra	interleukin-1 receptor antagonist
LP	lectin pathway
MBL	mannose-binding lectin
OGD	oxygen-glucose deprivation
2-PM	two-photon microscopy
RBC	red blood cell
tMCAo	transient middle cerebral artery occlusion
TMD1	thrombomodulin lectin-like domain
WT	wild-type

Platelets are key elements of thromboinflammatory cascades, and their role in inflammatory processes is increasingly recognized.[15–17] A mutual complement-platelet activation process exists in which both partners directly support each other in their functions.[18] Platelets express complement proteins and regulatory molecules, suggesting their susceptibility to complement activation,[18] although a specific role for LP has never been proposed.

Overall, available evidence suggests a role of LP in vascular inflammation and injury but a coherent picture of its effects in ischemic vessels cannot be drawn yet. By using in vivo, ex vivo, and in vitro approaches in wild-type (WT) and MBL genetically deficient mice and analyzing different time points post-injury, we have explored MBL actions on cerebral hemodynamics and inflammatory effects with the aim of understanding MBL-driven events after ischemic injury. We show here that MBL drives platelet inflammatory phenotype and release of IL-1α (interleukin-1α) early after ischemia. In turn, IL-1α acts as a trigger for MBL whose presence subsequently sustains the vascular pro-inflammatory phenotype, contributing to brain injury after stroke.

Materials and Methods

All data and materials have been made publicly available at the Figshare repository and can be accessed at doi:10.6084/m9.figshare.7007921.

Animals

Procedures involving animals and their care were conducted in conformity with institutional guidelines that are in compliance with national and international laws and policies. Male 9- to 11-week-old C57Bl/6J mice with target mutation of *MBL-A* and *MBL-C* genes (MBL$^{-/-}$, 26–28 g, purchased from Jackson Laboratories and colonized at Mario Negri Institute), IL-1αβ$^{-/-}$ and IL-1R1$^{-/-}$ mice,[19] and wild-type C57Bl/6J mice (WT, 25–28 g, used as the control strain as indicated in the strain datasheet for the mutated mice; visit https://www.jax.org/strain/006122) were used. The experiments on IL-1Ra (interleukin-1 receptor antagonist)-treated (100 mg/kg via subcutaneous injection) and IL-1 αβ$^{-/-}$ mice and respective WT controls were done under appropriate United Kingdom Home Office licenses and adhered to the Animals (Scientific Procedures) Act (1986). The protocols and details of this report are in accordance with ARRIVE guidelines (Animal Research: Reporting In Vivo Experiments; http://www.nc3rs.org.uk/page.asp?id=1357; check list provided in the online-only Data Supplement). We used

only male mice since estrogens affect the ischemic outcome in experimental models.[20] The study of the hormonal contribution to the ischemic lesion was beyond this work's purposes, for example, exploring the mechanisms of MBL-driven endothelial damage.

Surgery Protocols

Transient Middle Cerebral Artery Occlusion
Transient middle cerebral artery occlusion (tMCAo) was induced with a siliconized filament (7-0, Doccol Corporation) introduced into the right carotid artery and advanced to block the origin of middle cerebral artery (MCA) for 30 minutes, as described previously.[6,21] Surgery-associated mortality rate was 7%. See also online-only Data Supplement. Surgery and treatment protocols used for IL-1Ra-treated and IL-1 αβ$^{-/-}$ mice and respective WT controls are described previously.[22]

Cranial Window for Two-Photon Imaging
Mice were isoflurane-anesthetized with rectal temperature maintained at 37°C and positioned on a stereotactic frame (KOPF, CA). A cranial window was opened at AP: −1 mm and L: −2.5 mm from bregma to expose vessels in the region fed by the MCA.[23,24] After a midline scalp incision, the periostium was gently removed and a round cranial window (2.3 mm in diameter, wide enough to uncover the distal branches of the MCA) was performed. Mice were allowed an overnight recovery before the first imaging session. See also online-only Data Supplement.

Two-Photon Microscopy

Image Acquisition
Craniotomized mice were kept under gaseous anesthesia (1.5% isoflurane in a mixture of O_2/NO_2, 30/70 %) during imaging. Images were acquired with a BX51WI microscope coupled to an FV300 scanner head (Olympus Corporation, Tokyo, Japan), equipped with a multiphoton laser, Chamaleon ultra II (Coherent, Santa Clara). Vessels were labeled by intravenous injection of rhodamine-dextran (RhITC, Sigma Aldrich; 70 kDa, 2.5% in sterile water, 120 μL). Pial and penetrating arterioles were acquired over a volume sized 800×600×200 μm. The acquisition volume was placed within the first 300 μm below the dura mater, in an area which is susceptible to the ischemic injury induced by tMCAo.[23] The penetrating arterioles that were analyzed had a portion parallel to the cortical surface before diving perpendicularly, thus allowing blood flow speed quantification[25] as described below. Details of acquisition protocol can be found in online-only Data Supplement.

Image Processing for Vessel Diameter, Blood Flow Speed, and Extravasation Measurements
All the vessels with diameter <45 μm were included in the following measurements obtained using Fiji software.[26] Further details on image processing can be found in online-only Data Supplement.

Vessel Lumen Diameter
A maximum projection image over the stack containing a given vessel was used to quantify labeled pixel length (=vessel lumen).

Blood Flow Speed
Blood flow speed was calculated as red blood cells (RBC) speed (mm/s) according to the line-scan method.[25] A negative value for speed indicates inversion of the blood flow from the baseline. Absolute values were used to quantify the percent of baseline value used for the statistical analysis.

Extravasation
Extravasation was identified by parenchymal accumulation of the fluorescent marker (which cannot cross the intact blood-brain barrier).[24] A mean projection image was obtained over the stack containing a given vessel. Extravasation was calculated as the ratio of intra- to extravascular pixel density. Scattered cells taking up the dye (possibly macrophages and astrocytes) were excluded from pixel

density calculation (Figure I in the online-only Data Supplement). All data are expressed as the-fold change from the pre-occlusion time.

Immunohistochemistry

Immunohistochemistry was done on 20 μm brain coronal cryosections using biotinylated anti-mouse ICAM-1 (intracellular adhesion molecule-1; 1 μg/mL; R&D Biosystems, No. 553251), rat anti-mouse CD206 (10 μg/mL; Serotec, Kidlington, No. MCA2235, UK), anti-mouse thrombomodulin (1 μg/mL; R&D Biosystems, No. MAB3894), and rat anti-mouse CD31 (0.16 μg/mL; BD Pharmigen, No. 550274). A secondary biotinylated antibody against rat was used. Positive cells were stained by reaction with 3,3 diaminobenzidine-tetrahydrochloride (Vector laboratories, CA). For negative control staining, the primary antibodies were omitted, and no staining was observed (Figure II in the online-only Data Supplement).

Slice Selection and Quantitative Analysis for Immunohistochemistry

Three brain coronal sections per mouse (+0.6, 0, and –0.6 mm from bregma[27]) were used for quantification of markers in striatum, representing the core of the lesion and cortex, representing the perilesional area/penumbra region. On each slice, anatomically defined striatal and cortical regions of interest were marked out, indicating regions in the territory fed by the MCA.[23] See also online-only Data Supplement and Figure III in the online-only Data Supplement. The immunostained areas for ICAM-1 and thrombomodulin, expressed as positive pixels/total assessed pixels (percentage area stained), number of CD206+ cells/mm^{2}, or density of grid touchings[28] for CD31 were measured using Fiji software and used for statistical analysis.[29]

Immunofluorescence

Immunofluorescence was done on 20-μm-thick coronal brain sections. After blockade with 2% normal donkey serum or BSA for 1 hour, sections were incubated in mixtures of rabbit anti-Iba1 (0.4 μg/mL; WAKO, No. PA5-48108), goat anti-IL-1α (2 μg/mL; RnDsystems, No. AF-400), rat anti-CD41 (5 μg/mL; BD Biosciences, No. 553847), rabbit anti-C3 (4 μg/mL; Santacruz, No. H-300 sc-20137), or rat anti-MBL-C (1 μg/mL; Hycult, No. HM1038) primary antibodies followed by appropriate Alexa 488- or Alexa 594-conjugated secondary antibodies raised in donkey or goat (4 μg/mL; Life Sciences). Blood vessels were visualized with biotinylated tomato lectin (Sigma, 10 μg/mL) followed by incubation with streptavidin Alexa 350-conjugated (2 μg/mL; Life Sciences) or *Griffonia Simplicifolia* isolectin B4 Alexa 488-conjugated (10 μg/mL; Life Sciences). For negative control staining, the primary antibodies were omitted, and no staining was observed (Figure II in the online-only Data Supplement). Confocal microscopy was done using a sequential scanning mode to avoid bleed-through effects with an Olympus FV500 microscope.[30] Three-dimensional volumes were acquired over 7 to 10 μm stacks, with 0.23 μm step size.[30] For the quantification of MBL-C staining, microphotographs were taken in the ischemic cortex (×40 magnification, pixel size 0.45 μm) and processed by ImageJ. Briefly, a region of interest was delineated on the IB4 signal (blood vessels). The region of interest was then applied to the corresponding image with the MBL-C signal after appropriate normalization (the background noise was corrected by subtracting the mean pixel density of unstained areas). The integrated density was calculated and used for statistical analysis. For the assessment of microglial IL-1α production, double immunofluorescence (using rabbit-anti Iba1 and goat anti-IL-1α antibodies, see above) was performed. IL-1α-positive microglia were counted in the ipsilateral hemisphere (2 randomly selected fields of view taken from 3-3 coronal brain sections in each mouse using fixed coordinates defined according to bregma). For the immunofluorescence on platelets, these cells were collected from WT ischemic mice at 6 hours after tMCAo as previously described.[31] Platelets were then primed in Tyrode's buffer containing 1 mmol/L CaCl$_2$ and incubated for 30 minutes at 37°C with 1/10 (v/v in Tyrode's buffer) plasma pooled from 3 tMCAo 6-hour mice. Three microliter of the platelet suspension were spotted on a gelatinized glass to run immunofluorescence

with rat anti-mouse MBL-A or MBL-C (both 1 μg/mL; Hycult, No. HM1035 and No. HM1038, respectively) followed by Alexa 546-conjugated secondary antibody raised in goat (4 μg/mL; Life Sciences) and FITC-conjugated phalloidin (7.5 U/mL; Life Sciences). Confocal microscopy was done with a sequential scanning mode with a Nikon A1 system (×100 magnification, pixel size 0.1 μm).

Western Blot Analysis

Blood samples were collected in 10 mmol/L ethylendiaminetetracetic acid and 0.125% polybrene (Sigma-Aldrich), and plasma was separated and stored at −80°C. Plasma proteins (10 μg/sample) were electrophoresed and transferred to polyvinylidene fluoride membranes. Rat anti-thrombomodulin monoclonal antibody (10 μg/mL; R&D, No. MAB3894) or rabbit anti-C3 polyclonal (2 μg/mL; Santa Cruz Biotechnology, No. H-300 sc-20137) followed by anti-rat or anti-rabbit peroxidase-conjugated antibodies (respectively, 0.04 μg/mL or 0.16 μg/mL; Santa Cruz Biotechnology). Quantifications were done using Quantity 1 Software (Bio-Rad), and results were standardized using the total protein loaded (Ponceau solution, Bio-Rad).

Cytokine Measurement

Platelets and blood cells were lysed in ice-cold buffer (50 mmol/L Tris-HCl pH 7.4, 150 mmol/L NaCl, 5 mmol/L CaCl$_2$, 0.02% NaN$_3$, 1% Triton X) containing protease inhibitors (Calbiochem) for 30 minutes followed by centrifugation for 10 minutes at 15 000g. Mouse, IL-1α and CXCL1 (chemokine [C-X-C motif] ligand 1) were measured with DuoSet ELISA kits (R & D Systems) according to the manufacturer's protocol. Protein concentrations were calculated with BCA assay (Pierce, Thermo-Fisher Scientific).

Platelet Activation Assay

Platelets were isolated from the right cardiac ventricle of anesthetized male C57BL/6 mice as previously described.[31] The platelets were resuspended in Tyrode's buffer and exposed to 10 μg/mL recombinant MBL (R&D) with or without 1 mmol/L CaCl$_2$ and incubated at 37°C for 30 minutes. Platelets were labeled with CD62P-APC and CD42d-PE antibodies (both 0.5 μg/mL; eBioscience, No. 17-0626-82 and No. 12-0421-82, respectively) for 5 minutes before flow cytometric analysis using a BD FACSVerse instrument (BD Biosciences).

Human Brain Microvascular Endothelial Cells and Oxygen-Glucose Deprivation

Human brain microvascular endothelial cells (hBMECs; Innoprot) were cultured on fibronectin-coated (15 μg/mL) black 96-well μ-plates (ibidi cell in focus, Germany) in basal medium supplemented with fetal bovine serum, endothelial cell growth cocktail, and penicillin/streptomycin solution (Innoprot). In vitro ischemia was induced by 5 hours oxygen-glucose deprivation (OGD) as previously described.[32]

To assess the role of platelets in vitro, platelets were gathered from WT and MBL$^{-/-}$ naive mice (n=8/10) as previously described[31] and pooled in separate vials for each genotype. After the OGD period, hBMECs were incubated with normoglycemic modified medium with or without WT or MBL$^{-/-}$ platelets (145×10^3 cells/well).

Cell Death Measurement

Forty-eight hours after OGD, hBMECs were incubated with propidium iodide fluorescent dye (5 μg/mL; Sigma-Aldrich). Propidium iodide incorporation was measured with a spectrofluorimeter (λ_{exc}=535 nm, λ_{em}=617 nm; TECAN plate reader, Infinite M200, Switzerland). Cells were then fixed for 30 minutes at room temperature with 4% paraformaldehyde. Nuclei were stained with 4′-6-diamidino-2-phenylindole (1 μg/mL; Invitrogen), and fluorescence was measured with a spectrofluorimeter (λ_{exc}=355 nm, λ_{em}=458 nm). Cell death was expressed as propidium iodide over 4′-6-diamidino-2-phenylindole fluorescence for each well.

Experimental Design, Blinding, and Exclusion Criteria

In each experiment, WT and MBL^{−/−} mice were randomly allocated to surgery groups taking care to distribute them equally across experimental days to avoid systematic errors. All subsequent evaluations were made by blinded investigators. Animals with no deficits during the occlusion period or with subarachnoid hemorrhage detected after brain removal were excluded from the study (3% of total tMCAo animals).

Statistical Analysis

Comparisons among groups were done by ANOVA and post hoc test as indicated in each figure legend. The parametric or nonparametric test was selected after a Kolmogorov-Smirnov test for normality to assess whether groups met normal distribution. The constancy of variances was checked by Bartlett test. Welch's corrected 1-way ANOVA followed by Games-Howell test was used for normally distributed data with unequal variances (Figures 2A, 3A, 4C, 5A, 5D′, 5F, and 5G). Group size was defined as the following formula: $n=2\sigma 2f(\alpha,\beta)/\Delta 2$ (SD in groups=σ, type 1 error α=0.05, type II error β=0.2, percentage difference between groups Δ=30). For each measure, the SD between groups was calculated on the basis of previous experiments with the same output parameters (eg, for stained area quantification σ=19, yielding n=6.34).

Statistical analysis was done using standard software packages GraphPad Prism (GraphPad Software Inc, San Diego, CA; version 6.0); *P* values <0.05 were considered significant.

Please see the Major Resources Table in online-only Data Supplement for further details.

Results

MBL Deficiency Ameliorates Impaired Hemodynamic Responses After Ischemia

In vivo 2-photon microscopy (2-PM) was used to measure brain hemodynamics in WT or MBL^{−/−} ischemic mice. Two-PM in vivo imaging sessions were done longitudinally at selected time points (Figure 1A): before (pre), 1 hour (post-1 hour), and 24 hours (post-24 hours) after the onset of ischemia, induced by tMCAo. Two-PM imaging was performed over the cortical region fed by the MCA, for example, where blood flow is reduced and cell death occurs.[23] The acquired volumes (Figure 1B) were used to measure RBC speed, extravasation, and vessel lumen diameter at the selected times. As expected, both WT and MBL^{−/−} mice had significant drops in RBC speed 1 hour after ischemia. However, at post-24 hours, MBL^{−/−} mice showed significantly better blood flow recovery than WT mice, the latter showing a further reduction in RBC speed at this time point (Figure 1C). WT and MBL^{−/−} mouse vessels had comparable extravasation of the fluorescent dye at 1 hour post-ischemia, but MBL^{−/−} mice had significantly less extravasation than WT mice at post-24 hours, indicating an earlier improvement of blood-brain barrier leakage (Figure 1C). WT mouse vessels indeed had a progressive increase in extravasation over time up to post-24 hours. Data on extravasation refer to a cortical region near to the brain surface as 2-PM imaging was limited to the first 300 µm below the dura mater; thus, deeper parenchymal leakage from brain capillaries was not measured. Conversely, the contribution of subarachnoid space bleeding cannot be excluded.

Both WT and MBL^{−/−} mice showed no significant changes in vessel lumen diameter after ischemia compared to the pre time point—likely due to the effect of isoflurane which was used as anesthetic[33]—and no difference between genotypes (Figure 1C) thus showing that the reported changes were not due to changes in diameter. Moreover, WT and MBL^{−/−} had no differences in RBC speed, vessel lumen diameter, and flux rate before ischemia (pre; Table I in the online-only Data Supplement), and previous studies demonstrated no genotype differences in cerebrovascular anatomy.[34] We can therefore exclude that the hemodynamic differences observed between the 2 genotypes depend on different local vasodilatation or on strain differences in blood flow or vessel anatomy.

WT and MBL^{−/−} sham mice had no differences in vessel diameter and blood flow speed at any of the time points analyzed (Figure IV in the online-only Data Supplement).

MBL Deficiency Induces a Shift From a Pro- to an Anti-Inflammatory Vascular Phenotype in Ischemic Brain Areas
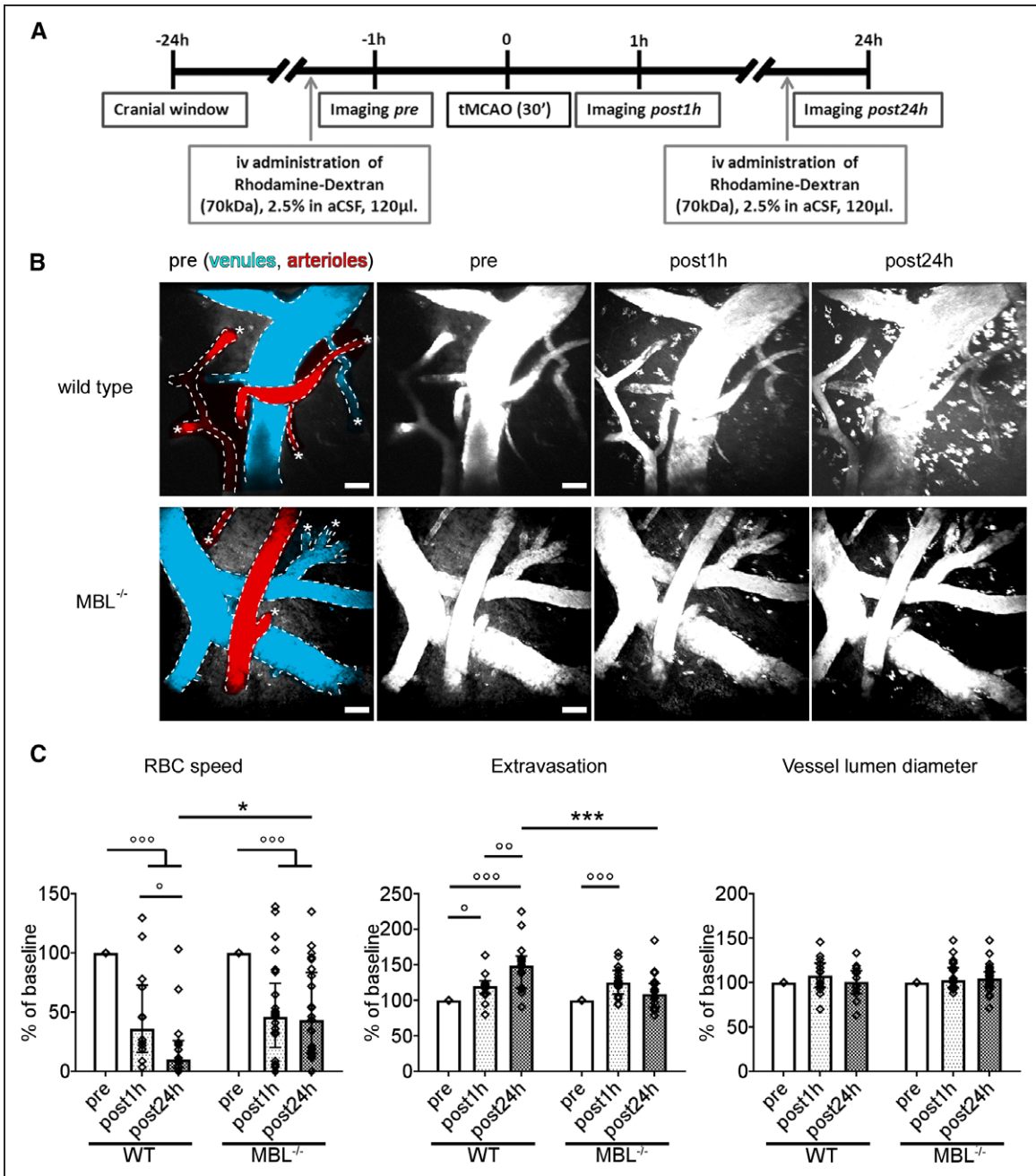
Since MBL deficiency ameliorates impaired hemodynamic responses after ischemia, suggesting an attenuation of vascular inflammatory responses, we assessed measures of vascular inflammation and function.

Assessment of C3 fragments, that result from C3 enzymatic cleavage, and of its deposition on the ischemic tissue are index of complement activation. Twenty-four hours after tMCAo, ischemic MBL^{−/−} mice had lower C3b plasma levels than ischemic WT mice, indicating an attenuated complement systemic activation (Figure 2A and complete Western blot experiment shown in Figure V in the online-only Data Supplement), consistent with MBL role as initiator molecule of LP of complement activation. In addition, locally, immunofluorescent analysis of C3 protein showed that MBL^{−/−} mice (Figure 2B′) had less C3 deposited on the ischemic cortical area than WT (Figure 2B). C3 appeared located close to vessels pertinent to the ischemic area.

ICAM-1, a protein expressed by activated endothelial cells and involved in the recruitment of inflammatory cells to the injured brain,[35,36] was undetectable in both strains in naive mice, but it increased over time after tMCAo in striatum and cortex (respectively, *P*=0.0002 and *P*=0.0164; Figure 3A and 3B). Notably, ischemic MBL^{−/−} mice had lower ICAM-1 expression in striatum than ischemic WT mice 24 hours after tMCAo (Figure 3A). No differences between ischemic WT and MBL^{−/−} mice were found in cortex, where the staining intensity was weak (Figure 3B).

CD206-positive perivascular macrophages, which represent a resident macrophage subset involved in permeability control and blood-brain barrier integrity,[37] were on the contrary increased as a consequence of MBL deletion. CD206-positive cells increased with time after ischemia in striatum and cortex (*P*=0.0003 and *P*=0.0022, respectively; Figure 3C and 3D). MBL^{−/−} mice had a higher number of CD206-positive cells than WT mice in striatum and cortex 24 hours after tMCAo (Figure 3C and 3D).

To further explore the consequences of MBL deficiency on vascular inflammation, we then focused on thrombomodulin, an anti-inflammatory protein expressed on the surface of endothelial cells which also acts as a negative regulator of complement activation.[38] Six hours after ischemia,
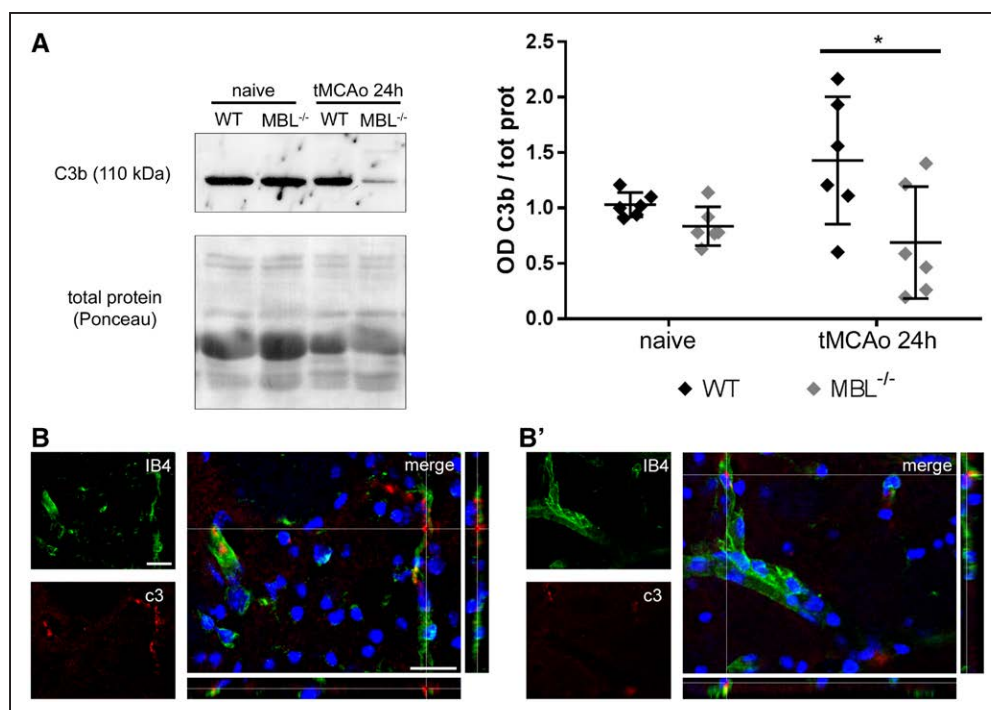
Figure 1. MBL (mannose-binding lectin) deficiency ameliorates impaired hemodynamic responses after ischemia as assessed by in vivo 2-photon microscopy. **A**, Wild type (WT) or MBL$^{-/-}$ mice underwent craniotomy and in vivo imaging before (pre), 1 h (post-1 h), and 24 h (post-24 h) after ischemic onset. **B**, Representative images of the acquired volume at each time point for WT and MBL$^{-/-}$ mice from a ventral perspective. Vessels are labeled by rhodamine-dextran injected systemically, pseudocolored in red and blue to depict arterioles and venules, respectively, at pre. Asterisks indicate penetrating capillaries. Rhodamine-dextran is shown also in white to compare each time point. Both strains showed a significant drop in red blood cells (RBC) speed at post-1 h, but MBL$^{-/-}$ had better flow recovery than WT at post-24 h (**C**). In both strains extravasation appeared at post-1 h, but MBL$^{-/-}$ showed less extravasation than WT at post-24 h (**C**). Both strains had no significant changes in vessel lumen diameter after ischemia compared with pre, with no differences between genotypes (**C**). Individual vessel changes (% of pre) are plotted (n=14–25 vessels from 4 mice per strain). Data are expressed as aligned dot plot with bars at median±interquartile range; 2-way repeated measures (RM) ANOVA followed by Sidak post hoc test; °$P<0.05$, °°$P<0.01$, °°°$P<0.001$; *$P<0.05$, ***$P<0.001$.

thrombomodulin expression was significantly reduced in the striatum and in cortex of both strains (surgery effect, striatum: $P=0.0002$; cortex: $P<0.0001$; Figure 4A and 4B). However, 24 hours after ischemia, this anti-inflammatory protein was significantly higher in the cortex of MBL$^{-/-}$ than in WT mice (Figure 4B). Thrombomodulin cleavage product (thrombomodulin-lectin domain, TMD1) can be shed and found in

blood as a circulating protein. Twenty-four hours after ischemia, MBL$^{-/-}$ mice had significantly higher levels of circulating TMD1 compared with WT mice (Figure 4C and complete Western blot experiment shown in Figure V in the online-only Data Supplement).

Vessel density, measured by CD31 staining, did not differ between the 2 groups (for tMCAo mice at 24 hours, striatum:

Figure 2. MBL (mannose-binding lectin) deficiency attenuates complement activation. Western blot analysis of C3b fragments in plasma of wild-type (WT) and MBL$^{-/-}$ naive or ischemic mice 24 h after transient middle cerebral artery occlusion (tMCAo) showed that ischemic MBL$^{-/-}$ mice have less circulating C3b fragments after tMCAo (**A**; the complete gel with all samples is shown in Figure V in the online-only Data Supplement). Data are expressed as scatter dot plot with line at mean±SD, n=6; Welch corrected 1-way ANOVA followed by Games-Howell test, *$P<0.05$. Immunostaining in the ischemic cortex shows that C3 (red) is present close to vessels (green) in WT (**B**) and MBL$^{-/-}$ (**B′**) mice, the latter showing less deposition. Nuclei are in blue, scale bars=20 μm.

912.1±68.5 for WT versus 945.1±175.9 for MBL$^{-/-}$; cortex 869.0±84.6 for WT versus 985.6±251.0 for MBL$^{-/-}$, density expressed as grid touchings per mm^2; Figure VI in the online-only Data Supplement), indicating that the reported differences in the vascular expression of the above-mentioned molecules were not due to different vessel density in the 2 genotypes.

At 24 hours after injury, the ischemic lesion did not differ between the 2 genotypes (19.76±5.10 versus 20.54±6.99 mm^3, mean±SD; Figure VII in the online-only Data Supplement).

MBL Deficiency Selectively Lowers IL-1α Expression in Platelets

IL-1 is a major pro-inflammatory cytokine produced by both microglia and peripheral immune cells that drives ICAM-1 expression on cerebral microvessels.[31] Since hematopoietic IL-1 contributes to brain injury and vascular inflammation after cerebral ischemia[39] and platelets are an important source of IL-1α,[31] we measured IL-1α levels in different cell types 6 hours after tMCAo. Platelets from MBL$^{-/-}$ mice had lower IL-1α expression levels than those from WT mice (Figure 5A). In contrast, blood cells pelleted from whole blood or microglia in the brain did not show any difference in IL-1α expression in the 2 genotypes (Figure 5B). Since platelet aggregation is associated with a greater brain injury,[40] we investigated whether MBL$^{-/-}$ mice presented differences in the number of platelet aggregates in cerebral microvessels compared with WT. We found no differences in platelet aggregates between the genotypes (Figure VIII in the online-only Data Supplement). Importantly, we found that platelets

are capable of binding MBL on their surface, as evidenced by immunoreactivity of platelets for both MBL murine isoforms after incubation with plasma from 6-hour tMCAo mice (Figure 5C). To test whether this interaction could drive platelet activation, we isolated platelets from naive WT mice and incubated them with recombinant MBL (10 μg/mL) for 30 minutes with or without the addition of 1 mmol/L CaCl$_2$. CaCl$_2$ alone induced a slight (not significant) increase in platelet activation, while MBL significantly increased platelet activation in the presence of CaCl$_2$. In contrast, MBL alone (ie, in the absence of CaCl$_2$) did not induce platelet activation (Figure 5D and 5D′).

Platelets From MBL$^{-/-}$ Mice Attenuate OGD-Induced CXCL1 Release and Death Compared to Platelets From WT Mice in hBMEC

Next, we checked whether MBL would induce platelets to alter their inflammatory profile after hypoxia/ischemia. Since platelets drive vascular inflammation via IL-1α,[31] we investigated whether MBL deficiency contributed to the weaker endothelial injury after ischemia through platelet-mediated responses. Cultured hBMECs monolayers were exposed to 5 hours OGD or left under normoxic conditions. hBMECs were then incubated 48 hours with vehicle medium or platelets from WT or MBL$^{-/-}$ mice (145×10^3 cells/well; Figure 5E). Cultured medium from OGD-hBMECs exposed to MBL$^{-/-}$ platelets had lower levels of CXCL1 than OGD-hBMEC exposed to WT platelets (Figure 5F). hBMEC cell death was significantly greater after the OGD insult compared with normoxic condition, irrespective of treatment (Figure 5G). However, OGD
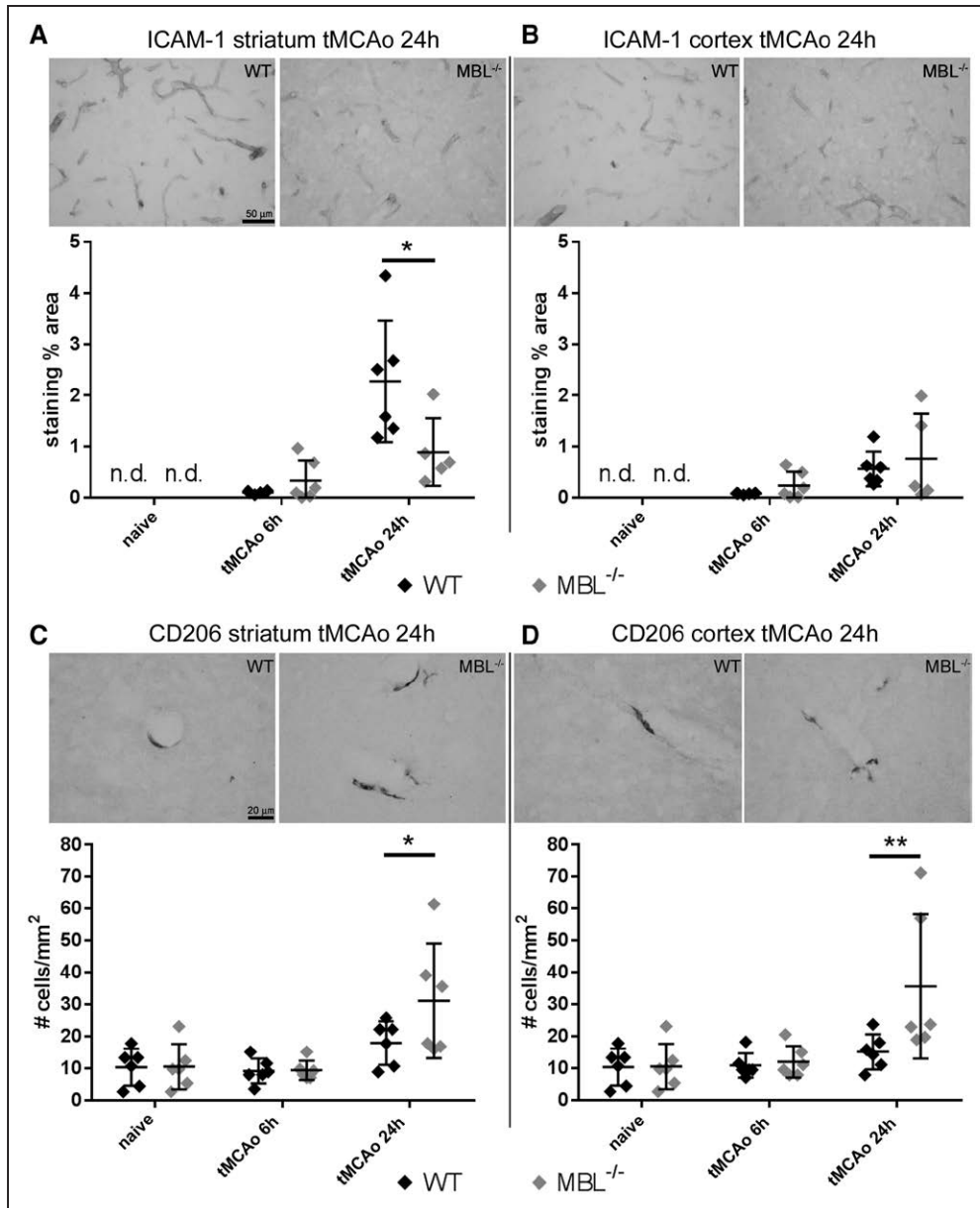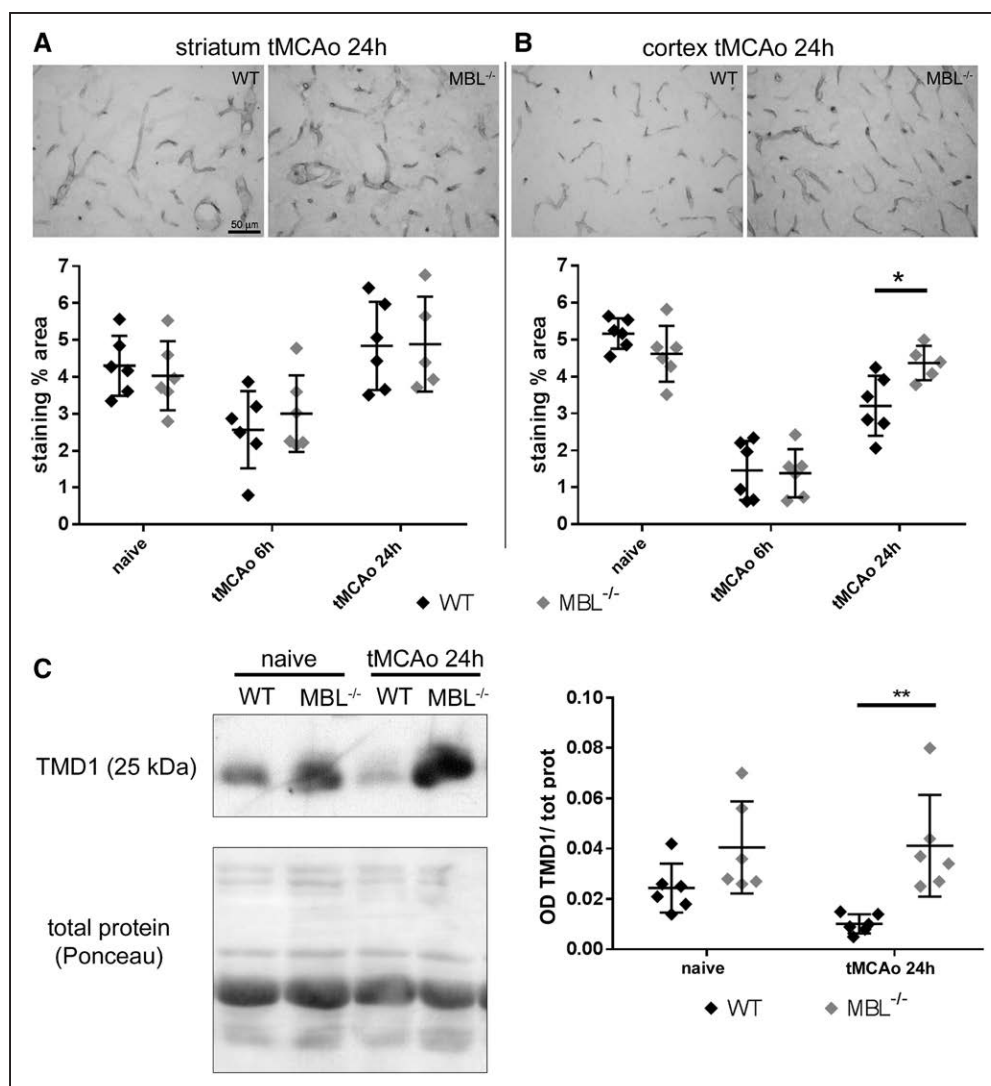
Figure 3. MBL (mannose-binding lectin) deficiency reduces ICAM-1 (intracellular adhesion molecule-1) and raises CD206 expression in ischemic brain areas. Representative images of ICAM-1 staining in striatum (**A**) or cortex (**B**) of wild-type (WT) and MBL$^{-/-}$ mice 24 h after transient middle cerebral artery occlusion (tMCAo) (bar=50 μm). ICAM-1 was detectable only in ischemic mice in both strains. Twenty-four hours after tMCAo MBL$^{-/-}$, mice had lower expression of ICAM-1 than WT mice in striatum (**A**). Representative images of CD206 staining in striatum (**C**) or cortex (**D**) of WT and MBL$^{-/-}$ mice 24 h after tMCAo (bar=20 μm). At this time point, MBL$^{-/-}$ ischemic mice had a higher number of CD206$^+$ cells in striatum (**C**) and cortex (**D**) than WT mice. Data are expressed as scatter dot plot with line at mean±SD, n=5–6; Welch corrected 1-way ANOVA followed by Games-Howell test for ICAM-1, *$P<0.05$; 2-way ANOVA followed by Sidak's post hoc test for CD206 (surgery effect $P=0.0003$ for striatum and $P=0.0022$ for cortex, not shown); *$P<0.05$, **$P<0.01$. nd=not detectable.

hBMECs exposed to MBL$^{-/-}$ platelets had significantly less cell death than those exposed to WT platelets (Figure 5G).

Blockade of IL-1 Signaling Decreases MBL Deposition on Ischemic Vessels 24 Hours After Ischemia

Mice deficient for IL-1αβ or those treated with IL-1Ra show markedly reduced brain injury after cerebral ischemia.[41–43] To investigate the interplay between MBL and IL-1-related pathways, we measured MBL deposition in the ischemic area of WT mice treated with the competitive IL-1R1 (IL-1

receptor 1) antagonist, IL-1Ra (100 mg/kg, subcutaneously), or with vehicle, in IL-1αβ knock out (IL-1αβ$^{-/-}$) and in IL-1 receptor 1 knock out (IL-1R1$^{-/-}$) mice, 24 hours after tMCAo, a time point when deposition is maximal.[6] Mice treated with IL-1Ra showed a significant 59%, IL-1αβ$^{-/-}$ mice a 47% and IL-1R1$^{-/-}$ mice a 48% decrease of MBL deposition on the ischemic vessels compared with controls (Figure 6). Thus, beyond its direct actions on brain microvessels and neurons,[41] IL-1 released from platelets seems also to augment vascular injury and subsequent brain damage by facilitating vascular MBL deposition after cerebral ischemia.

Figure 4. MBL (mannose-binding lectin) deficiency increases thrombomodulin expression and its shedded circulating lectin domain (TMD1). Representative images of thrombomodulin staining in striatum (**A**) and cortex (**B**) of wild-type (WT) and MBL$^{-/-}$ mice 24 h after transient middle cerebral artery occlusion (tMCAo; bar = 50 µm). At this time point, MBL$^{-/-}$ ischemic mice had higher thrombomodulin expression in cortex than WT ischemic mice (**B**). Data are expressed as scatter dot plot with line at mean±SD, n=5–6; 2-way ANOVA followed by Sidak's post hoc test (surgery effect P=0.0002 for striatum and P<0.0001 for cortex, not shown); *P<0.05, **P<0.01. Quantitative analysis of thrombomodulin immunoblot indicated that 24 h after tMCAo, MBL$^{-/-}$ mice had higher levels of thrombomodulin lectin-domain (TMD1, 25 kDa) in plasma than WT mice (**C**; the complete gel with all samples is shown in Figure V in the online-only Data Supplement). Data are expressed as scatter dot plot with line at mean±SD, n=6 Welch corrected 1-way ANOVA followed by Games-Howell test, **P<0.01.

Discussion

This study shows that MBL drives vascular responses after cerebral ischemia through platelet-derived IL-1α, thus proposing a previously unexplored mechanism of detrimental complement actions after stroke. In particular, MBL seems to promote an inflammatory phenotype in platelets early after ischemia. Platelet IL-1α, in turn, favor MBL deposition on the ischemic vessels, sustaining the vascular inflammatory phenotype that ultimately drives the ischemic lesion expansion. Thus, MBL- and IL-1-mediated actions interact to establish vascular inflammatory responses and brain injury after cerebral ischemia.

Both MBL and IL-1 deficiency are associated with smaller brain injury and better functional outcome after cerebral ischemia.[5,6,39,41] Here we report better hemodynamics and an attenuated endothelial inflammatory phenotype in MBL$^{-/-}$ mice 24 hours after ischemia. At this time point, WT and MBL$^{-/-}$ have similar lesion volume, ruling out the possibility that the effects of MBL deletion described here at 24 hours are secondary to the reduced injury. As previously published by us and others,[5,6] MBL$^{-/-}$ mice show smaller lesion volume at 48 hours after insult, thus suggesting that MBL activates secondary mechanisms which contribute to lesion expansion. The similar ischemic lesion that we observed at 24 hours in our model does not contradict previous findings reporting a significant protection at 24 hours in MBL$^{-/-}$ mice when using a stronger ischemic insult, for example, 90′ tMCAo and showing a wider lesion size at this time point (lesion volume ≈50 mm³).[34]

Available evidence supports that MBL deficiency is associated with better reperfusion after ischemia.[34] Here we
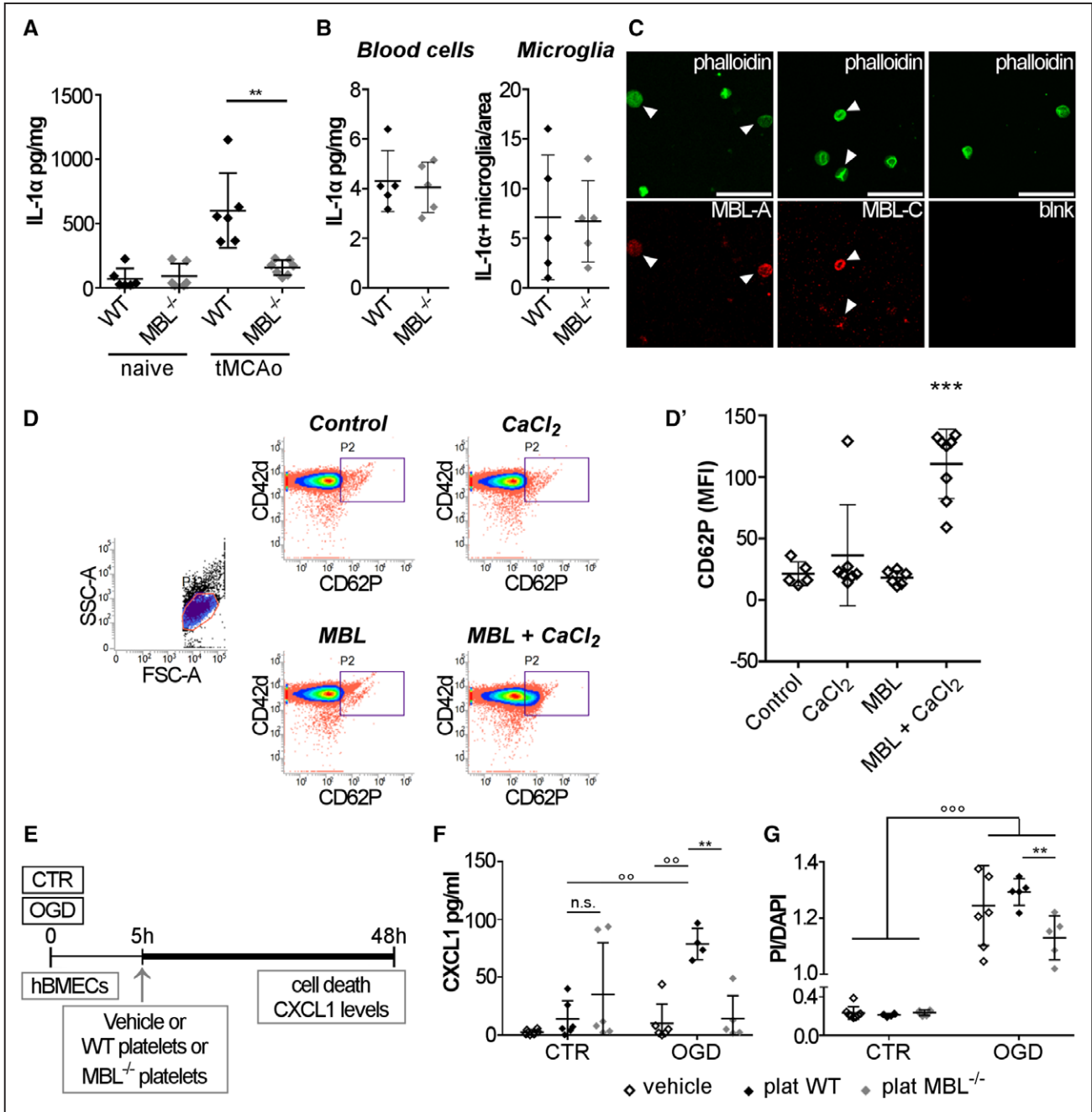
Figure 5. MBL (mannose-binding lectin) deficiency selectively lowers IL-1α (interleukin-1α) expression in platelets which induce less CXCL1 (chemokine [C-X-C motif] ligand 1) release and less cell death in vitro when exposed to human brain microvascular endothelial cells (hBMECs) subjected to oxygen-glucose deprivation (OGD.) Six hours after transient middle cerebral artery occlusion (tMCAo), IL-1α content was significantly reduced in platelets (**A**) but not in other blood cells or in microglia (**B**) from MBL⁻/⁻ mice compared with wild-type (WT) mice. Data are expressed as scatter dot plot with line at mean±SD, n=6; Welch corrected 1-way ANOVA followed by Games-Howell test, **P<0.01. Platelets extracted from ischemic WT mice and incubated with murine plasma were clearly positive for MBL-A and MBL-C (**C**; arrowheads, the right panel shows the negative control for the immunostaining, bars=20 μm). Platelets from naive WT mice showed significant activation (increased CD62P levels) when incubated for 30 min with MBL in the presence of CaCl2 (representative cytometric density plots in **D** and quantification in **D′**). Data are expressed as scatter dot plot with line at mean±SD, n=5–8, Welch corrected 1-way ANOVA followed by Games-Howell test, ***P<0.001 vs control. Platelets obtained from MBL⁻/⁻ mice when incubated with hBMECs subjected to OGD (**E**) induced lower CXCL1 release (**F**) and less cell death (**G**) than those obtained from WT mice. Data are expressed as scatter dot plot with line at mean±SD, n=6, Welch corrected 1-way ANOVA followed by Games-Howell test, **P<0.01, °°°P<0.001, °°P<0.01.

show by in vivo 2-PM that MBL⁻/⁻ mice have better vascular function than WT mice 24 hours after ischemia, with faster blood flow and lower extravasation values. The attenuation of vascular dysfunction is not apparent early after the insult (1 hour), implying that the observed effects are not due to genetic

changes in the vasculature, but rather to MBL activation of secondary mechanisms affecting vascular function. In vivo 2-PM, high resolution allows to study individual vessels over time. In MBL⁻/⁻ ischemic mice, we observed better function of small vessels with a diameter smaller than 45 μm, which are
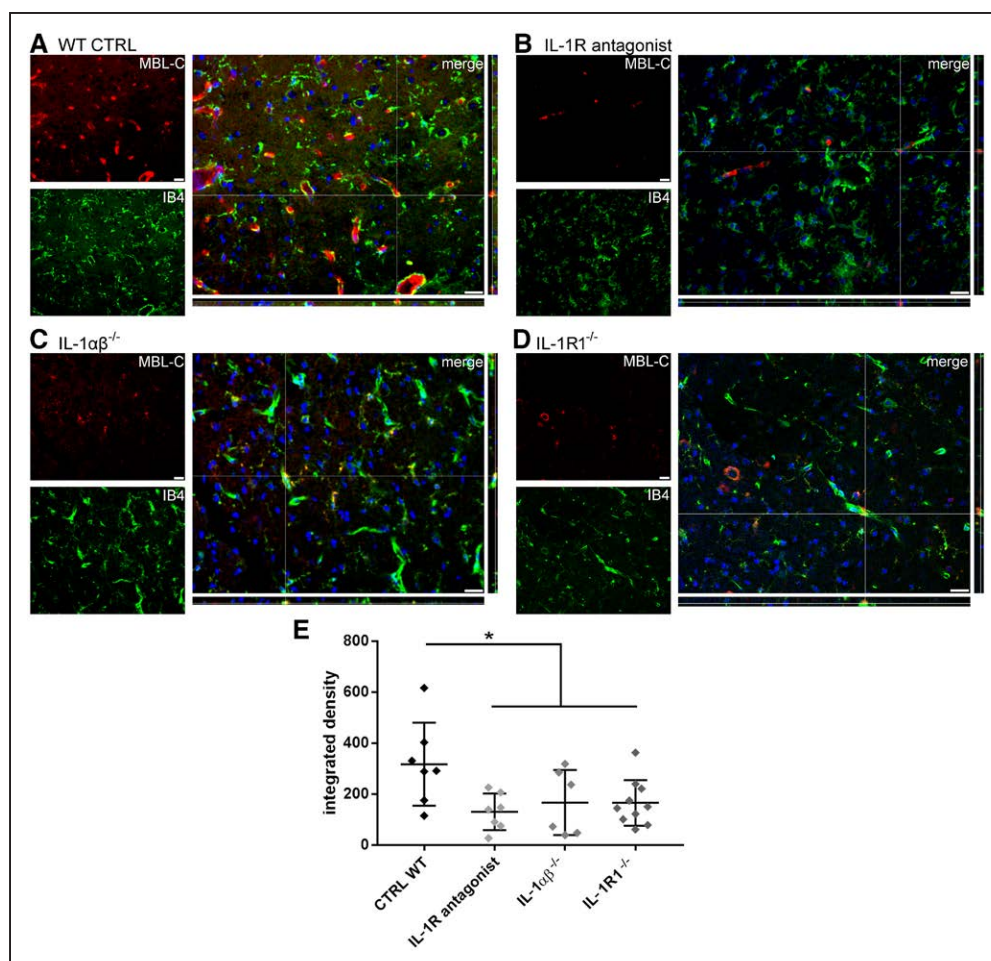
Figure 6. IL-1 (interleukin-1) receptor 1 (IL-1R) inhibition decreases MBL (mannose-binding lectin) deposition on ischemic vessels 24 h after ischemia. Representative images of MBL-C (red) and vessels (IB4, green) from wild-type (WT; **A**), IL-1R antagonist-treated (**B**), IL-1αβ^{−/−} (**C**), or IL-1R1^{−/−} (**D**) mice (bars=20 μm). The fluorescence intensity of MBL-C staining (integrated density) was decreased in IL-1R antagonist-treated, IL-1αβ^{−/−} and IL-1R1^{−/−} compared with WT mice (**E**). Data are expressed as scatter dot plot with line at mean±SD, n=6–10; 1-way ANOVA followed by Holm-Sidak's post hoc test, *$P < 0.05$.

believed to be the most susceptible to secondary blood clotting. Events of no-reflow are indeed typical of small vessels[36] and can have a great effect on brain viability.[44] Well-known secondary pathogenic mechanisms include fibrin and platelet deposits,[31,45,46] local vasoconstriction caused by pericytes,[47] and deposition of intravascular clusters of immune cells during their recruitment,[24] all events promoting secondary clots and driving focal no-reflow.[36]

MBL deficiency–related amelioration of hemodynamic responses after ischemia improved vascular inflammatory response, showing an overall shift from a pro-inflammatory to an anti-inflammatory phenotype, for example, decreased C3b (complement activation[48]) and endothelial ICAM-1 (an adhesion molecule which facilitates leukocyte endothelial transmigration).

Interestingly, CD206-positive macrophages increased in the ischemic area of MBL^{−/−} mice, indicating that MBL deletion favors a protective and anti-inflammatory environment. These macrophages are located at the interface between vessels and brain parenchyma as they patrol the albuminal space of the cerebral vasculature. They act by limiting vessel leakage[37] and inflammation, promoting prohealing processes after brain

damage,[49] similarly to other M2 polarized myeloid cells.[50] MBL deficiency was also associated with increased endothelial expression of the anticoagulant and anti-inflammatory protein thrombomodulin and with increased circulating levels of its fragment TMD1.[51] Thrombomodulin anchors to the luminal side of the vascular endothelial cell membrane, exerting physiological control of blood flow.[52] Among its several anti-inflammatory actions, thrombomodulin prevents excessive blood clotting by inhibiting the conversion of fibrinogen into fibrin by thrombin.[10,38] The observed increase in endothelial-bound thrombomodulin 24 hours after ischemia therefore suggests an antithrombotic profile of the endothelium in MBL^{−/−} mice. The N-terminus end of thrombomodulin may be cleaved into short 25 kDa fragments containing a lectin-like domain (TMD1), which may directly bind HMGB1 (high mobility group box 1) and prevent the activation of RAGE on endothelial cells.[38,53] TMD1 also modulate the expression of ICAM-1 and VCAM-1 (vascular cell adhesion molecule 1)[51]. In addition, and relevant for our study, TMD1 may negatively regulate the complement system.[54] In our study, TMD1 plasmatic concentrations in MBL^{−/−} ischemic mice significantly increased compared with WT mice 24 hours after injury. This

is consistent with an anti-inflammatory role of TMD1 after ischemia and suggests that MBL can downregulate TMD1 production, resulting in an enhanced inflammatory vascular phenotype. The TMD1 increase in MBL$^{-/-}$ ischemic mice may explain the observed tendency in C3b level drop after ischemia in these mice. This hypothesis is in line with the reported ability of TMD1 to negative complement regulation,[54] although we acknowledge that other unknown mechanisms may be involved in this effect.

The improvement in hemodynamics and the changes in vascular inflammatory response in MBL$^{-/-}$ ischemic mice were evident 24 hours after injury, with no change at earlier times (1 hour and 6 hours, respectively). To further explore events occurring early after ischemia and possibly explain later events, 6 hours after ischemic onset, we measured inflammatory cytokines in different cellular compartments. We found that 6 hours after ischemia platelets (but not other blood cells or microglia) had a dramatically lower IL-1α content compared with WT mice. IL-1α released by platelets has a critical role in inflammation-mediated injury in the brain.[31] In fact, it induces the endothelial expression of ICAM-1, VCAM-1, and CXCL1, besides enhancing neutrophil trans-endothelial migration, all well-known mechanisms of brain damage after injury.[31,55–57]

We show here for the first time that murine platelets bind MBL, and high MBL levels may facilitate platelet activation in a calcium-dependent manner, implying a direct involvement of platelets in MBL-driven pathological effects. We thus tested whether MBL deficiency contributed to the reduced endothelial injury after ischemia through platelet-mediated responses. Consistent with our hypothesis, hBMEC subjected to OGD and incubated with platelets from MBL$^{-/-}$ mice showed significantly reduced release of CXCL1, a chemokine whose release is driven by platelet

IL-1α,[31] than platelets from WT. In line with the pro-inflammatory function of platelets in ischemic injury, our overall data define for the first time a role of MBL in inducing IL-1α release from platelets. Our data indicate that this is an early consequence of ischemia (6 hours), impacting on vessel viability over the first 24 hours and possibly leading to neuronal injury by 48 hours.[6] Counteracting IL-1α release by MBL deletion results in preserved microvessel function 24 hours after ischemia.

Further supporting the link between MBL and IL-1α, genetic deletion of IL-1 or its receptor and IL-1R antagonism reduced MBL deposition 24 hours after ischemia, a time when high MBL deposition is expected.[6] These mice were also protected from the ischemic injury, having smaller lesion size and decreased vascular permeability,[43] further supporting the key role of this pathway in driving vascular damage.

Conclusions

In this study, we show that MBL deficiency is associated with decreased cerebrovascular dysfunctions and endothelial pro-inflammatory phenotype after brain ischemia, compared with controls, and propose a central role for platelet IL-1α in MBL-mediated endothelial damage.

The detrimental effects of MBL depend at least in part on its interaction with platelets. As a working hypothesis (Figure 7), we propose that early after ischemia (6 hours), circulating MBL drives platelet activation. Active platelets release IL-1α that on binding to its receptor (IL-1R1) causes vascular inflammation, facilitating vascular injury. Later on, 24 hours after injury, damaged endothelial cells induce MBL deposition triggering complement activation (cleaved C3) and favoring a pro-inflammatory activation of the endothelium (ICAM-1) to the detriment of protective functions (CD206 and thrombomodulin and TMD1). Therefore, MBL contributes to
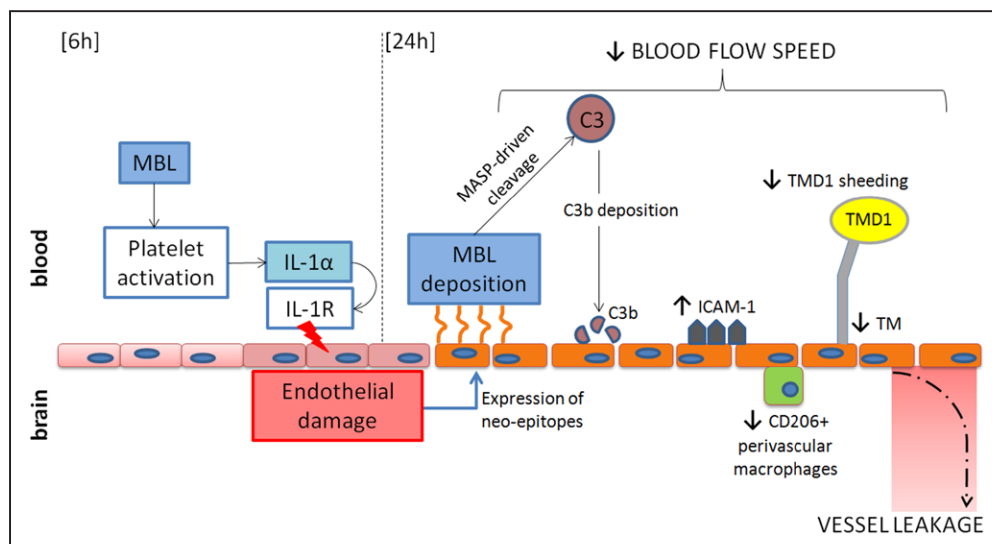
Figure 7. MBL (mannose-binding lectin) and IL-1α (Interleukin-1α) interplay on the ischemic endothelium and its consequences. Early after ischemia (6 h), circulating MBL drives platelet activation by a direct action on platelets. Actived platelets release IL-1α, which on binding to its receptor (IL-1R) contributes to endothelial damage.[31] Damaged endothelial cells drive MBL deposition,[6] which results in complement activation, increase of ICAM-1 (intracellular adhesion molecule-1) expression on vessels, favoring focal no-reflow,[36] decrease of thrombomodulin (TM) expression on the endothelium and of its circulating shedded domain (TMD1), all effects indicative of vascular inflammation, and decrease of CD206-positive perivascular macrophages in the brain, a population involved in blood-brain barrier (BBB) structural maintenance.[37] All these events contribute to reduction of blood flow speed and increase of BBB leakage observed after the ischemic insult.

the final ischemic injury by activating detrimental cascades on the ischemic endothelium within 24 hours, which may kick off subsequent inflammatory pathways.

We propose MBL as a hub of pathogenic vascular events. The interaction with IL-1α is indeed one of the possible pathways by which MBL exerts its detrimental role after ischemia. However, we acknowledge that these effects may be linked to other molecular interactions, or to direct endothelial damage induced by MBL deposition as reported in few in vitro studies using renal peritubular epithelial cells,[58] or colorectal carcinomal cells.[59]

Disclosures

None.

References

1. Pedersen ED, Løberg EM, Vege E, Daha MR, Maehlen J, Mollnes TE. In situ deposition of complement in human acute brain ischaemia. *Scand J Immunol*. 2009;69:555–562. doi:10.1111/j.1365-3083.2009.02253.x

2. Mocco J, Mack WJ, Ducruet AF, Sosunov SA, Sughrue ME, Hassid BG, Nair MN, Laufer I, Komotar RJ, Claire M, Holland H, Pinsky DJ, Connolly ES Jr. Complement component C3 mediates inflammatory injury following focal cerebral ischemia. *Circ Res*. 2006;99:209–217. doi: 10.1161/01.RES.0000232544.90675.42

3. Orsini F, De Blasio D, Zangari R, Zanier ER, De Simoni MG. Versatility of the complement system in neuroinflammation, neurodegeneration and brain homeostasis. *Front Cell Neurosci*. 2014;8:380. doi: 10.3389/fncel.2014.00380

4. Gesuete R, Storini C, Fantin A, Stravalaci M, Zanier ER, Orsini F, Vietsch H, Mannesse ML, Ziere B, Gobbi M, De Simoni MG. Recombinant C1 inhibitor in brain ischemic injury. *Ann Neurol*. 2009;66:332–342. doi: 10.1002/ana.21740

5. Cervera A, Planas AM, Justicia C, Urra X, Jensenius JC, Torres F, Lozano F, Chamorro A. Genetically-defined deficiency of mannose-binding lectin is associated with protection after experimental stroke in mice and outcome in human stroke. *PLoS One*. 2010;5:e8433. doi: 10.1371/journal.pone.0008433

6. Orsini F, Villa P, Parrella S, et al. Targeting mannose-binding lectin confers long-lasting protection with a surprisingly wide therapeutic window in cerebral ischemia. *Circulation*. 2012;126:1484–1494. doi: 10.1161/CIRCULATIONAHA.112.103051

7. Osthoff M, Katan M, Fluri F, Schuetz P, Bingisser R, Kappos L, Steck AJ, Engelter ST, Mueller B, Christ-Crain M, Trendelenburg M. Mannose-binding lectin deficiency is associated with smaller infarction size and favorable outcome in ischemic stroke patients. *PLoS One*. 2011;6:e21338. doi: 10.1371/journal.pone.0021338

8. Collard CD, Väkevä A, Morrissey MA, Agah A, Rollins SA, Reenstra WR, Buras JA, Meri S, Stahl GL. Complement activation after oxidative stress: role of the lectin complement pathway. *Am J Pathol*. 2000;156:1549–1556. doi: 10.1016/S0002-9440(10)65026-2

9. Collard CD, Montalto MC, Reenstra WR, Buras JA, Stahl GL. Endothelial oxidative stress activates the lectin complement pathway: role of cytokeratin 1. *Am J Pathol*. 2001;159:1045–1054. doi: 10.1016/S0002-9440(10)61779-8

10. Bossi F, Peerschke EI, Ghebrehiwet B, Tedesco F. Cross-talk between the complement and the kinin system in vascular permeability. *Immunol Lett*. 2011;140:7–13. doi: 10.1016/j.imlet.2011.06.006

11. Kenawy HI, Boral I, Bevington A. Complement-coagulation cross-talk: a potential mediator of the physiological activation of complement by low pH. *Front Immunol*. 2015;6:215. doi: 10.3389/fimmu.2015.00215

12. Fumagalli S, De Simoni MG. Lectin complement pathway and its bloody interactions in brain ischemia. *Stroke*. 2016;47:3067–3073. doi: 10.1161/STROKEAHA.116.012407

13. Zhao XJ, Larkin TM, Lauver MA, Ahmad S, Ducruet AF. Tissue plasminogen activator mediates deleterious complement cascade activation in stroke. *PLoS One*. 2017;12:e0180822. doi: 10.1371/journal.pone.0180822

14. Jenny L, Dobó J, Gál P, Pál G, Lam WA, Schroeder V. MASP-1 of the complement system enhances clot formation in a microvascular whole blood flow model. *PLoS One*. 2018;13:e0191292. doi: 10.1371/journal.pone.0191292

15. Chen C, Li T, Zhao Y, Qian Y, Li X, Dai X, Huang D, Pan T, Zhou L. Platelet glycoprotein receptor Ib blockade ameliorates experimental cerebral ischemia-reperfusion injury by strengthening the blood-brain barrier function and anti-thrombo-inflammatory property. *Brain Behav Immun*. 2017;69:255–263. doi:10.1016/j.bbi.2017.11.019

16. Cloutier N, Allaeys I, Marcoux G, et al. Platelets release pathogenic serotonin and return to circulation after immune complex-mediated sequestration. *Proc Natl Acad Sci USA*. 2018;115:E1550–E1559. doi: 10.1073/pnas.1720553115

17. Salas-Perdomo A, Miró-Mur F, Urra X, Justicia C, Gallizioli M, Zhao Y, Brait VH, Laredo C, Tudela R, Hidalgo A, Chamorro Á, Planas AM. T cells prevent hemorrhagic transformation in ischemic stroke by P-selectin binding [published online June 14, 2018]. *Arterioscler Thromb Vasc Biol*. doi:10.1161/ATVBAHA.118.311284

18. Speth C, Rambach G, Würzner R, Lass-Flörl C, Kozarcanin H, Hamad OA, Nilsson B, Ekdahl KN. Complement and platelets: mutual interference in the immune network. *Mol Immunol*. 2015;67:108–118. doi: 10.1016/j.molimm.2015.03.244

19. Horai R, Asano M, Sudo K, Kanuka H, Suzuki M, Nishihara M, Takahashi M, Iwakura Y. Production of mice deficient in genes for interleukin (IL)-1alpha, IL-1beta, IL-1alpha/beta, and IL-1 receptor antagonist shows that IL-1beta is crucial in turpentine-induced fever development and glucocorticoid secretion. *J Exp Med*. 1998;187:1463–1475.

20. Carswell HVO, Macrae IM, Farr TD. Complexities of oestrogen in stroke. *Clin Sci (Lond)*. 2009;118:375–389. doi:10.1042/CS20090018

21. De Simoni MG, Rossi E, Storini C, Pizzimenti S, Echart C, Bergamaschini L. The powerful neuroprotective action of C1-inhibitor on brain ischemia-reperfusion injury does not require C1q. *Am J Pathol*. 2004;164:1857–1863. doi:10.1016/S0002-9440(10)63744-3

22. Pradillo JM, Murray KN, Coutts GA, Moraga A, Oroz-Gonjar F, Boutin H, Moro MA, Lizasoain I, Rothwell NJ, Allan SM. Reparative effects of interleukin-1 receptor antagonist in young and aged/co-morbid rodents after cerebral ischemia. *Brain Behav Immun*. 2017;61:117–126. doi: 10.1016/j.bbi.2016.11.013

23. Fumagalli S, Perego C, Ortolano F, De Simoni MG. CX3CR1 deficiency induces an early protective inflammatory environment in ischemic mice. *Glia*. 2013;61:827–842. doi: 10.1002/glia.22474

24. Fumagalli S, Ortolano F, De Simoni MG. A close look at brain dynamics: cells and vessels seen by in vivo two-photon microscopy. *Prog Neurobiol*. 2014;121:36–54. doi: 10.1016/j.pneurobio.2014.06.005

25. Shih AY, Driscoll JD, Drew PJ, Nishimura N, Schaffer CB, Kleinfeld D. Two-photon microscopy as a tool to study blood flow and neurovascular coupling in the rodent brain. *J Cereb Blood Flow Metab*. 2012;32:1277–1309. doi: 10.1038/jcbfm.2011.196

26. Schindelin J, Arganda-Carreras I, Frise E, et al. Fiji: an open-source platform for biological-image analysis. *Nat Methods*. 2012;9:676–682. doi: 10.1038/nmeth.2019

27. Franklin KBJ, Paxinos G. *The Mouse Brain in Stereotaxic Coordinates*. Academic Press.

28. Pischiutta F, D'Amico G, Dander E, Biondi A, Biagi E, Citerio G, De Simoni MG, Zanier ER. Immunosuppression does not affect human bone marrow mesenchymal stromal cell efficacy after transplantation in traumatized mice brain. *Neuropharmacology*. 2014;79:119–126. doi: 10.1016/j.neuropharm.2013.11.001

29. Perego C, Fumagalli S, De Simoni MG. Temporal pattern of expression and colocalization of microglia/macrophage phenotype markers following brain ischemic injury in mice. *J Neuroinflammation*. 2011;8:174. doi: 10.1186/1742-2094-8-174

30. Perego C, Fumagalli S, De Simoni M-G. Three-dimensional confocal analysis of microglia/macrophage markers of polarization in experimental brain injury. *J Vis Exp*. 2013:e50605. doi:10.3791/50605

31. Thornton P, McColl BW, Greenhalgh A, Denes A, Allan SM, Rothwell NJ. Platelet interleukin-1alpha drives cerebrovascular inflammation. *Blood*. 2010;115:3632–3639. doi: 10.1182/blood-2009-11-252643

32. Gesuete R, Orsini F, Zanier ER, Albani D, Deli MA, Bazzoni G, De Simoni MG. Glial cells drive preconditioning-induced blood-brain barrier protection. *Stroke*. 2011;42:1445–1453. doi:10.1161/STROKEAHA.110.603266

33. Santisakultarm TP, Kersbergen CJ, Bandy DK, Ide DC, Choi SH, Silva AC. Two-photon imaging of cerebral hemodynamics and neural activity in awake and anesthetized marmosets. *J Neurosci Methods*. 2016;271:55–64. doi:10.1016/j.jneumeth.2016.07.003

34. de la Rosa X, Cervera A, Kristoffersen AK, Valdés CP, Varma HM, Justicia C, Durduran T, Chamorro Á, Planas AM. Mannose-binding lectin promotes local microvascular thrombosis after transient brain ischemia in mice. *Stroke*. 2014;45:1453–1459. doi:10.1161/STROKEAHA.113.004111

35. Gauberti M, Montagne A, Quenault A, Vivien D. Molecular magnetic resonance imaging of brain-immune interactions. *Front Cell Neurosci*. 2014;8:389. doi: 10.3389/fncel.2014.00389

36. del Zoppo GJ, Mabuchi T. Cerebral microvessel responses to focal ischemia. *J Cereb Blood Flow Metab*. 2003;23:879–894. doi: 10.1097/01.WCB.0000078322.96027.78

37. He H, Mack JJ, Güç E, Warren CM, Squadrito ML, Kilarski WW, Baer C, Freshman RD, McDonald AI, Ziyad S, Swartz MA, De Palma M, Iruela-Arispe ML. Perivascular macrophages limit permeability. *Arterioscler Thromb Vasc Biol*. 2016;36:2203–2212. doi: 10.1161/ATVBAHA.116.307592

38. Li YH, Kuo CH, Shi GY, Wu HL. The role of thrombomodulin lectin-like domain in inflammation. *J Biomed Sci*. 2012;19:34. doi: 10.1186/1423-0127-19-34

39. Denes A, Wilkinson F, Bigger B, Chu M, Rothwell NJ, Allan SM. Central and haematopoietic interleukin-1 both contribute to ischaemic brain injury in mice. *Dis Model Mech*. 2013;6:1043–1048. doi: 10.1242/dmm.011601

40. Dénes Á, Pradillo JM, Drake C, Sharp A, Warn P, Murray KN, Rohit B, Dockrell DH, Chamberlain J, Casbolt H, Francis S, Martinecz B, Nieswandt B, Rothwell NJ, Allan SM. Streptococcus pneumoniae worsens cerebral ischemia via interleukin 1 and platelet glycoprotein Ibα. *Ann Neurol*. 2014;75:670–683. doi: 10.1002/ana.24146

41. Denes A, Pinteaux E, Rothwell NJ, Allan SM. Interleukin-1 and stroke: biomarker, harbinger of damage, and therapeutic target. *Cerebrovasc Dis*. 2011;32:517–527. doi: 10.1159/000332205

42. McCann SK, Cramond F, Macleod MR, Sena ES. Systematic review and meta-analysis of the efficacy of interleukin-1 receptor antagonist in animal models of stroke: an update. *Transl Stroke Res*. 2016;7:395–406. doi: 10.1007/s12975-016-0489-z

43. Maysami S, Wong R, Pradillo JM, Denes A, Dhungana H, Malm T, Koistinaho J, Orset C, Rahman M, Rubio M, Schwaninger M, Vivien D, Bath PM, Rothwell NJ, Allan SM. A cross-laboratory preclinical study on the effectiveness of interleukin-1 receptor antagonist in stroke. *J Cereb Blood Flow Metab*. 2016;36:596–605. doi: 10.1177/0271678X15606714

44. Nishimura N, Schaffer CB. Big effects from tiny vessels: imaging the impact of microvascular clots and hemorrhages on the brain. *Stroke*. 2013;44(6 suppl 1):S90–S92. doi: 10.1161/STROKEAHA.112.679621

45. Davalos D, Ryu JK, Merlini M, et al. Fibrinogen-induced perivascular microglial clustering is required for the development of axonal damage in neuroinflammation. *Nat Commun*. 2012;3:1227. doi: 10.1038/ncomms2230

46. Kleinschnitz C, Pozgajova M, Pham M, Bendszus M, Nieswandt B, Stoll G. Targeting platelets in acute experimental stroke: impact of glycoprotein Ib, VI, and IIb/IIIa blockade on infarct size, functional outcome, and intracranial bleeding. *Circulation*. 2007;115:2323–2330. doi: 10.1161/CIRCULATIONAHA.107.691279

47. Fernández-Klett F, Offenhauser N, Dirnagl U, Priller J, Lindauer U. Pericytes in capillaries are contractile in vivo, but arterioles mediate functional hyperemia in the mouse brain. *Proc Natl Acad Sci USA*. 2010;107:22290–22295. doi: 10.1073/pnas.1011321108

48. Longhi L, Orsini F, De Blasio D, Fumagalli S, Ortolano F, Locatelli M, Stocchetti N, De Simoni MG. Mannose-binding lectin is expressed after clinical and experimental traumatic brain injury and its deletion is protective. *Crit Care Med*. 2014;42:1910–1918. doi: 10.1097/CCM.0000000000000399

49. Fumagalli S, Perego C, Pischiutta F, Zanier ER, De Simoni MG. The ischemic environment drives microglia and macrophage function. *Front Neurol*. 2015;6:81. doi: 10.3389/fneur.2015.00081

50. David S, Kroner A. Repertoire of microglial and macrophage responses after spinal cord injury. *Nat Rev Neurosci*. 2011;12:388–399. doi: 10.1038/nrn3053

51. Conway EM, Van de Wouwer M, Pollefeyt S, Jurk K, Van Aken H, De Vriese A, Weitz JI, Weiler H, Hellings PW, Schaeffer P, Herbert JM, Collen D, Theilmeier G. The lectin-like domain of thrombomodulin confers protection from neutrophil-mediated tissue damage by suppressing adhesion molecule expression via nuclear factor kappaB and mitogen-activated protein kinase pathways. *J Exp Med*. 2002;196:565–577.

52. Wu KK. TM hidden treasure: lectin-like domain. *Blood*. 2012;119:1103–1104. doi:10.1182/blood-2011-12-394544

53. Abeyama K, Stern DM, Ito Y, Kawahara K, Yoshimoto Y, Tanaka M, Uchimura T, Ida N, Yamazaki Y, Yamada S, Yamamoto Y, Yamamoto H, Iino S, Taniguchi N, Maruyama I. The N-terminal domain of thrombomodulin sequesters high-mobility group-B1 protein, a novel antiinflammatory mechanism. *J Clin Invest*. 2005;115:1267–1274. doi: 10.1172/JCI22782

54. Delvaeye M, Noris M, De Vriese A, Esmon CT, Esmon NL, Ferrell G, Del-Favero J, Plaisance S, Claes B, Lambrechts D, Zoja C, Remuzzi G, Conway EM. Thrombomodulin mutations in atypical hemolytic-uremic syndrome. *N Engl J Med*. 2009;361:345–357. doi: 10.1056/NEJMoa0810739

55. Pradillo JM, Denes A, Greenhalgh AD, Boutin H, Drake C, McColl BW, Barton E, Proctor SD, Russell JC, Rothwell NJ, Allan SM. Delayed administration of interleukin-1 receptor antagonist reduces ischemic brain damage and inflammation in comorbid rats. *J Cereb Blood Flow Metab*. 2012;32:1810–1819. doi: 10.1038/jcbfm.2012.101

56. Allen C, Thornton P, Denes A, McColl BW, Pierozynski A, Monestier M, Pinteaux E, Rothwell NJ, Allan SM. Neutrophil cerebrovascular transmigration triggers rapid neurotoxicity through release of proteases associated with decondensed DNA. *J Immunol*. 2012;189:381–392. doi: 10.4049/jimmunol.1200409

57. Giles JA, Greenhalgh AD, Denes A, Nieswandt B, Coutts G, McColl BW, Allan SM. Neutrophil infiltration to the brain is platelet-dependent, and is reversed by blockade of platelet GPIbα. *Immunology*. 2018;154:322–328. doi: 10.1111/imm.12892

58. van der Pol P, Schlagwein N, van Gijlswijk DJ, Berger SP, Roos A, Bajema IM, de Boer HC, de Fijter JW, Stahl GL, Daha MR, van Kooten C. Mannan-binding lectin mediates renal ischemia/reperfusion injury independent of complement activation. *Am J Transplant*. 2012;12:877–887. doi: 10.1111/j.1600-6143.2011.03887.x

59. Ma Y, Uemura K, Oka S, Kozutsumi Y, Kawasaki N, Kawasaki T. Antitumor activity of mannan-binding protein *in vivo* as revealed by a virus expression system: mannan-binding proteinindependent cell-mediated cytotoxicity. *Proc Natl Acad Sci USA*. 1999;96:371–375.

Highlights

- Mannose-binding lectin directly binds platelets inducing IL-1α (interleukin-1α) release.
- IL-1α favors mannose-binding lectin vascular deposition.
- Mannose-binding lectin deposition drives endothelial pro-inflammatory activation, thus contributing to brain injury.